PCCP

Cite this: *Phys. Chem. Chem. Phys.*, 2012, **14**, 14661–14666

www.rsc.org/pccp

PAPER

Solution-processed organic photovoltaic cells based on a squaraine dye†

Guo Chen,[a] Hisahiro Sasabe,*[a] Zhongqiang Wang,[a] Xiaofeng Wang,[a] Ziruo Hong,*[a] Junji Kido[a] and Yang Yang[b]

Received 18th July 2012, Accepted 29th August 2012
DOI: 10.1039/c2cp42445b

In this work, 2,4-bis[4-(*N*,*N*-diisobutylamino)-2,6-dihydroxyphenyl] squaraine (SQ) was systematically studied as an electron donor in solution processed photovoltaic cells, showing power conversion efficiency of >4.0% under AM1.5G 1 sun illumination at room temperature. Low mobilities were found to limit charge transport in the bulk heterojunctions. Efficiency was thus improved to 5.1% at 80 °C mainly due to improvement of photocurrent extraction. We also demonstrated that the SQ compound synthesized *via* a simple method has high purity, and thus can be used in photovoltaic cells without further purification. Our results suggest the huge potential of SQ and its analogs in organic photovoltaic applications.

1. Introduction

Significant progress in power conversion efficiency (η_p) and operational stability has been achieved from organic photovoltaic (OPV) cells. OPV technology has the potential applications for lightweight and flexible solar panels, and could be a cost-effective alternative for traditional solar cells in the future.[1]

So far, efficient OPV cells have been p–n junction devices based on organic p-type donor and n-type acceptor materials. Donor materials include polymer and small molecule materials, and acceptor materials are normally fullerenes and their derivatives. The basic requirements for OPV materials are strong absorption for light harvesting, suitable energy levels for exciton dissociation, and sufficient carrier mobility for charge collection.[2,3] Photoactive materials usually have extinction coefficients on the order of 1–2 × 10^5 cm^{-1}, resulting in sufficient light absorption in thin films of approximately 100 nm thickness. In such a scenario, photogenerated charge carriers can be extracted from bulk films having low carrier mobility of 10^{-2}–10^{-6} cm^2 V^{-1} s^{-1}.[4,5] Below this thickness, it is difficult to collect incident photons effectively, unless the photoactive materials have stronger absorption. Some squaraine compounds have exceptionally high extinction coefficients >3 × 10^5 cm^{-1},[6] with broad absorption bandwidth upon aggregation in solid films. As a result, thickness of photoactive layers can be as small as several tens of nanometers, while absorption is still significant. It is important, since small film thickness favors charge extraction. In spite of low carrier mobilities, squaraine compounds have been very attractive for use in OPVs recently.[7–14] For example, a squaraine layer with a thickness of merely 10 nm causes strong absorption and high photocurrent in OPV cells.

After synthesis of OPV materials, it takes further efforts for purification to ensure high PV performance.[15] Though remarkable progress has been made with respect to materials[16–19] and device architectures,[20–21] it would be desirable to explore alternative ways to circumvent the complicated and time-consuming purification processes. For instance, when a reaction ends, a proper molecular structure shall induce crystallization of the target compound, resulting in high purity. Molecular packing also benefits absorption in thin films. Here we demonstrated such an example using a squaraine compound, 2,4-bis[4-(*N*,*N*-diisobutylamino)-2,6-dihydroxyphenyl] squaraine (SQ), as a donor, and [6,6]-phenyl-C_{71}-butyric acid methyl ester ($PC_{70}BM$) as an acceptor in solution processed OPV cells, showing competitive PV performance in comparison with that based on 2-time sublimed SQ. Effects of donor/acceptor ratio (wt%) on PV performance were discussed over a large range from 1 : 1 up to 1 : 99. Furthermore it was found that high operational temperature enhanced η_p *via* improving carrier mobilities in the blend films.

2. Synthesis of the SQ compound

In general, polymers and oligomers as donor materials in OPV cells are prepared *via* palladium-catalyzed cross-coupling reaction. In such reactions, metal-catalysts, phosphine ligands, halogenated and toxic metal-containing compounds are typically used. Consequently, a considerable amount of by-products and residual catalysts/ligands remain in final products. It requires purification, since the contaminants generally have a negative influence on or even change the optoelectronic properties of the target products.[8]

[a] *Department of Organic Device Engineering, Graduate School of Science and Engineering, Research Center for Organic Electronics (ROEL), Yamagata University, 4-3-16 Jonan, Yonezawa, Yamagata 992-8510, Japan. E-mail: h-sasabe@yz.yamagata-u.ac.jp, ziruo@yz.yamagata-u.ac.jp*
[b] *Department of Materials Science and Engineering, University of California-Los Angeles, Los Angeles, CA 90095, USA*
† Electronic supplementary information (ESI) available. See DOI: 10.1039/c2cp42445b

From the synthesis point of view, SQ studied in this work has several advantages. (i) SQ is prepared *via* condensation reaction between electron-rich aromatic compounds and squaric acid, and thus the by-product is only water and easily removed *via* distillation; (ii) in this reaction, we do not use expensive and hardly-separable catalysts and ligands; (iii) the final SQ product has highly crystalline nature, and can form crystalline solids, which can be separated easily from the reaction mixture; (iv) the yield of the SQ product is as high as 80%. These features make SQ an attractive donor for OPVs.

SQ was synthesized using a modified method reported by Tian *et al.*[22]‡ In their paper, recrystallization of SQ from dichloromethane–methanol solution was carried out in the final step. On the other hand, Dirk *et al.* pointed out that the crystalline product formed *via* the reaction has purity >99% tested by 1H-NMR.[23] Thus the reaction mixture was filtered to collect SQ crystals, and then washed with organic solvents and dried *in vacuo*. We skipped recrystallization, and simply washed the SQ crystals with a mixture of methanol and hexanes. HPLC analysis confirmed the purity of the product to be >99.9% using THF–methanol (1 : 9) as eluents. The SQ product was also sublimated under high vacuum ($< 10^{-5}$ Pa), and the purities checked using elemental analysis (EA). There was negligible difference between as-synthesized and sublimated SQ. It is noteworthy that this synthetic route can be easily scaled up to the multigram level, *e.g.* ~10 g, offering low-cost materials for OPVs.

3. Results and discussion

3.1 Device fabrication and optimization

As shown in Fig. 1a, the SQ:$PC_{70}BM$ blend films were sandwiched between a molybdenum oxide (MoO_3) modified indium–tin-oxide (ITO) anode[24] and a bathocuproine (BCP)/Al cathode.[25] The energy level diagram is shown in Fig. 1b. An ITO/MoO_3 anode is necessary (Fig. S1 and Table SI, ESI†). MoO_3 effectively deepens the surface workfunction of ITO to −5.7 eV, and therefore delivers an open circuit voltage (V_{oc}) which corresponds to the highest occupied molecular orbital (HOMO) of the SQ compound of −5.3 eV.[9,26] Thickness of both MoO_3[27] and photoactive layers was optimized (see Fig. S2, ESI†).

The Fig. 2 inset shows absorption spectra of SQ and $PC_{70}BM$ neat films. SQ exhibits a broad band from 500 nm up to 750 nm, $PC_{70}BM$ covers near UV to green. Fig. 2 shows absorbance of SQ:$PC_{70}BM$ films with various blend ratios.

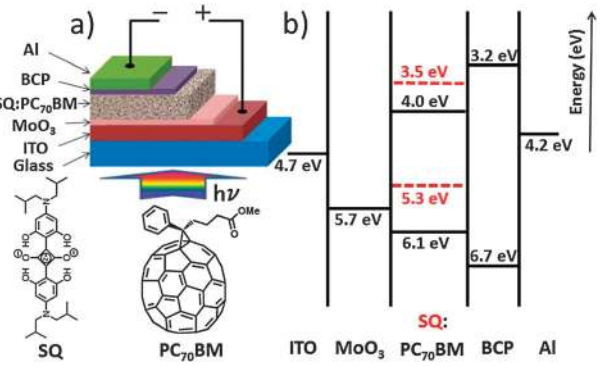

Fig. 1 Device architecture and molecular structures of photoactive materials (a), and corresponding energy diagram (b).

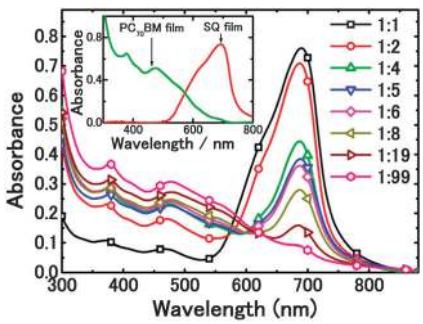

Fig. 2 Absorbance of SQ : $PC_{70}BM$ films with various blend ratios ranging from 1 : 1 to 1 : 99. The film thickness is approximately 70 ± 5 nm. The inset shows absorbance of solution-processed neat films of SQ and $PC_{70}BM$.

‡ Experimental section: synthesis of SQ compounds was carried out *via* a modified method reported by Tian and co-workers.[22] The aniline precursor was prepared according to their method. A mixture of aniline precursor (5.3 g, 22.3 mmol), squaric acid (1.14 g, 10.0 mmol), 1-butanol (50 mL), and toluene (150 mL) was nitrogen bubbled for 1 hour. Then, the resultant mixture was stirred for 6 hours at reflux temperature under N_2 flow with azeotropic distillation of water. After the mixture was concentrated to *ca.* 40 mL, cyclohexane (70 mL) was added to the reaction mixture. Then, the solvent (60 mL) was distilled again and the mixture was cooled to room temperature. The precipitate was filtered, and washed with methanol and hexanes, dried *in vacuo* to afford SQ (4.39 g, 79%) as shining green brown crystals. The purity of SQ was confirmed by HPLC analysis using THF–methanol (1 : 9) as eluents. The as-synthesized compound was sublimated twice using a high vacuum ($<10^{-5}$ Pa) system. Both as-synthesized and sublimated products were characterized by NMR, HPLC and elemental analysis. Data for as-synthesized SQ: HPLC (>99.9%), Anal. calcd for $C_{32}H_{44}O_6N_2$: C, 69.50; H, 8.02; N, 5.07%. Found: C, 69.62; H, 8.11; N, 5.03%. For sublimed SQ: HPLC (>99.9%), Anal. calcd for $C_{32}H_{44}O_6N_2$: C, 69.50; H, 8.02; N, 5.07%. Found: C, 69.54; H, 8.18; N, 4.99%. Device and thin film fabrication and characterization: patterned indium–tin-oxide (ITO) coated glass substrates were cleaned using detergent, de-ionized water, acetone and isopropanol in an ultrasonic bath. Cleaned substrates were dried and kept in an oven at 80 °C. Substrates were exposed to UV ozone for 30 min and immediately transferred into a high-vacuum chamber for deposition of 6 nm MoO_3 at a base pressure of 1×10^{-6} Pa. Photoactive layers (thickness: 70 ± 5 nm) were fabricated by spin-coating SQ:$PC_{70}BM$ solution (20 mg mL^{-1} in chloroform) on the MoO_3 coated ITO surface in the N_2-filling glove box, followed by thermal treatment at 70 °C for 10 min. The active layer of $PC_{70}BM$-only cells (70 ± 5 nm) was spin coated from $PC_{70}BM$ solution (20 mg mL^{-1} in chloroform) and then thermal annealed at 70 °C for 10 minutes. Finally, the substrates were transferred back to a high-vacuum chamber where BCP (10 nm) and Al (100 nm) were deposited as the top electrode. The active area of cells is 0.04 cm^2 defined by the overlap of the ITO anode and the Al cathode. The structures of hole-only and electron-only devices were ITO/MoO_3/SQ:$PC_{70}BM$/MoO_3/Al and ITO/Cs_2CO_3/SQ:$PC_{70}BM$/BCP/Al, respectively. *J–V* and EQE characterizations of PV cells were carried out on a CEP-2000 integrated system made by Bunkoukeiki Co. Bright state *J–V* characteristics were measured under simulated 100 mW cm AM1.5G irradiation from a Xe lamp with an AM1.5 global filter. EQE were measured with a Xe lamp, monochromator, chopper, and lock-in amplifier. The integration of EQE data over the AM1.5G solar spectrum yields calculated J_{sc} within 5% experimental difference from the measured J_{sc} under simulated solar light. UV-visible absorption spectra were obtained using a SHIMADZU MPC-2200 UV-visible spectrophotometer. Atomic force microscopy (AFM) was carried out on a Veeco AFM using a tapping mode.

Film thickness was kept at approximately 70 nm for fair comparison of absorbance and photovoltaic performance. With increasing loading of SQ, the absorption in long wavelength increases. For the films having a blend ratio of 1 : 4, 1 : 5, 1 : 6 and 1 : 8, absorbance of films reached 0.3. It is suggested that ~60% of incident photons within the absorption range can be absorbed according to the absorbance.[28]

Current density–voltage (J–V) characteristics of OPV cells under illumination of AM1.5G 100 mW cm^{-2} are shown in Fig. 3a and Table 1. Fig. 3b shows external quantum efficiency (EQE) spectra. For blending ratios of 1 : 4, 1 : 5 and 1 : 6, an average EQE over 50% was observed from 350 nm to 700 nm. 1 : 5 blending ratio yielded optimal η_p of 4.3%. The device shows V_{oc} of 0.94 V, consistent with the offset between the HOMO of SQ, and the lowest unoccupied molecular orbital (LUMO) of $PC_{70}BM$. A short circuit current (J_{sc}) of 10.8 mA cm^{-2} and a fill factor (FF) of 43% were obtained. Low FF indicates strong recombination in the OPV cells.

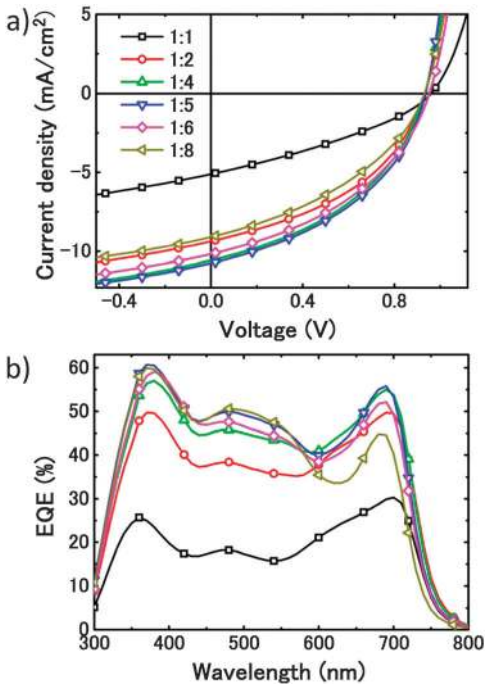

Fig. 3 (a) J–V characteristics illuminated at 100 mW cm^{-2} (AM1.5G solar spectrum) for the SQ : $PC_{70}BM$ cells at room temperature; (b) EQE curves of SQ : $PC_{70}BM$ cells of various blending ratios.

Table 1 Summary of the key parameters in the PV cells based on various SQ : $PC_{70}BM$ blend ratios and pure $PC_{70}BM$

Weight ratio	J_{sc} (mA cm^{-2})	V_{oc} (V)	FF	η_p (%) (P_0 = 100 mW cm^{-2})	η_{max}[a] (%)
1 : 1	5.0 ± 0.1	0.95 ± 0.01	0.31 ± 0.02	1.4 ± 0.2	1.9
1 : 2	9.2 ± 0.2	0.92 ± 0.01	0.41 ± 0.02	3.4 ± 0.3	5.7
1 : 4	10.4 ± 0.2	0.92 ± 0.01	0.41 ± 0.02	3.9 ± 0.3	5.7
1 : 5	10.6 ± 0.2	0.93 ± 0.01	0.41 ± 0.02	4.0 ± 0.3	6.2
1 : 6	10.0 ± 0.2	0.94 ± 0.01	0.40 ± 0.02	3.7 ± 0.3	5.1
1 : 8	8.9 ± 0.2	0.92 ± 0.01	0.37 ± 0.02	3.0 ± 0.3	4.5
1 : 19	5.7 ± 0.2	0.93 ± 0.01	0.33 ± 0.01	1.8 ± 0.1	2.7
1 : 99	2.0 ± 0.1	1.00 ± 0.01	0.27 ± 0.01	0.5 ± 0.1	0.86
$PC_{70}BM$	0.20 ± 0.02	1.22 ± 0.01	0.30 ± 0.01	0.07 ± 0.01	—

[a] Represents η_p under low incident light intensity of 3.5 mW cm^{-2}.

3.2 Light intensity dependence

Light intensity dependence of OPV performance is shown in Fig. 4. η_p of a 1 : 5 ratio PV cell increases from 4.3% at 100 mW cm^{-2} to 6.2% at 3.5 mW cm^{-2}. J_{sc} is linearly proportional to light intensity for all the cells. The slope values varied between 0.80 and 0.93, which deviate from 1.0, the ideal value for good PV cells. FF decreases with increasing incident light intensity, indicating that the recombination loss is sensitive to both electrical field and carrier density. As for V_{oc}, the slope varied significantly with donor/acceptor ratio. All PV cells show a sub-linear trend with saturation when light intensity reaches 1 sun. For blend ratios from 1 : 2 up to 1 : 8, the slope is roughly close to kT/q, indicating that bimolecular recombination dominates, where k is Boltzmann's constant, T is temperature, and q is elementary charge.[29] For other cases, *i.e.* 1 : 1, 1 : 19 and 1 : 99, the slope is larger than kT/q, suggesting that deep charge traps play a role.[30] J–V characteristics indicate that the 1 : 1 ratio cell has large serial resistance and high V_{oc}, indicating formation of space charge which prevents both collection and injection of carriers. The 1 : 19 and 1 : 99 cells with very low SQ loading ratio will be discussed in Section 3.6.

3.3 Effects of surface roughness

In bulk heterojunction OPV cells, film morphology often dominates the PV performance. AFM images of the blend films were taken using a tapping mode. Fig. 5 shows no significant domain formation in the films. Root-mean-square (RMS) roughness increases from 0.3 nm for the 1 : 1 case to 0.5 nm for 1 : 5, when $PC_{70}BM$ loading in the blend films increases. It coincides with the optimal η_p from the 1 : 5 ratio PV cell, meaning that aggregation of $PC_{70}BM$ occurs and favors electron transport. The 1 : 8 film had larger roughness, however, it delivered a lower η_p of 3.3% due to lower absorption of SQ. In polymer solar cells, the rough surface favors light harvesting and charge collection.[31] In our case, SQ:$PC_{70}BM$ blend films are thin and smooth. The smooth and uniform films are critical to avoid leakage current.

3.4 Temperature effects

Our investigation shows that SQ molecules do not form aggregation in the blend film. So in SQ:$PC_{70}BM$ films, carrier mobilities are expected to improve at elevated temperature.[32] Considering the outdoor working conditions of solar cells,[33] we tested our OPV cells at 80 °C. As shown in Fig. 6, compared to room temperature, both FF and J_{sc} increase, while V_{oc} slightly decreases at 80 °C. It results in almost 20% increase in η_p for all PV cells as summarized in Table 2. Note that after cooling down to room temperature, there is negligible change in the J–V characteristics in comparison with pristine devices. Absorption spectra (not shown) of the blend films also remain the same at temperature below 130 °C. Though temperature dependence of photovoltaic performance, especially V_{oc}, has been intensively studied in the OPV field,[34,35] normally efficiency changes little due to the compromise between V_{oc} and J_{sc}. In our case, 20% improvement in efficiency indicates the promising future of amorphous film based OPV cells, considering terrestrial application of solar panels.[36]

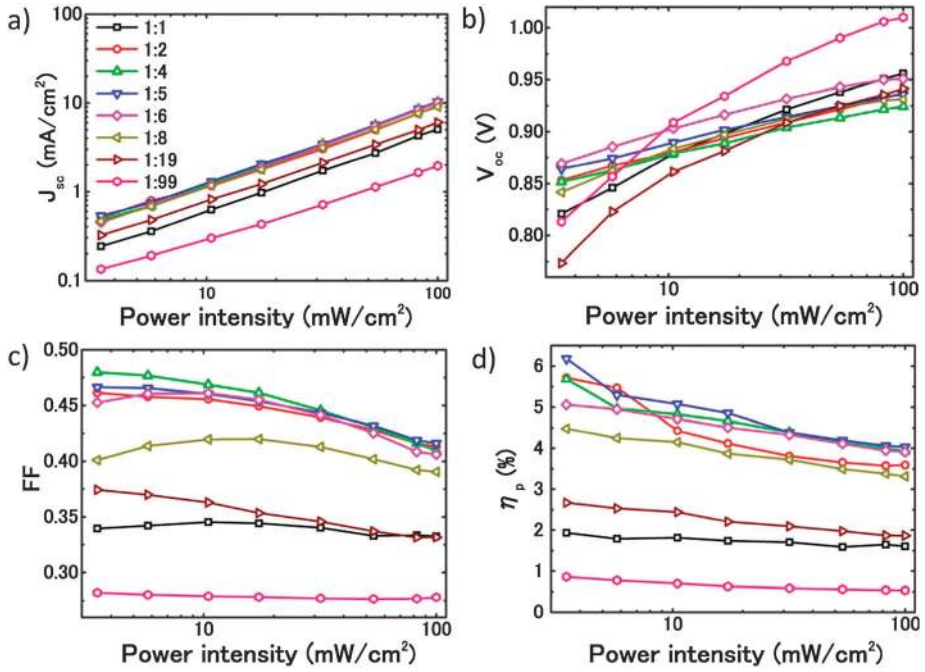

Fig. 4 (a) The short circuit current (J_{sc}), (b) open circuit voltage (V_{oc}), (c) fill factor and (d) power conversion efficiency (η_p) *versus* power intensity for the device with different blend ratios.

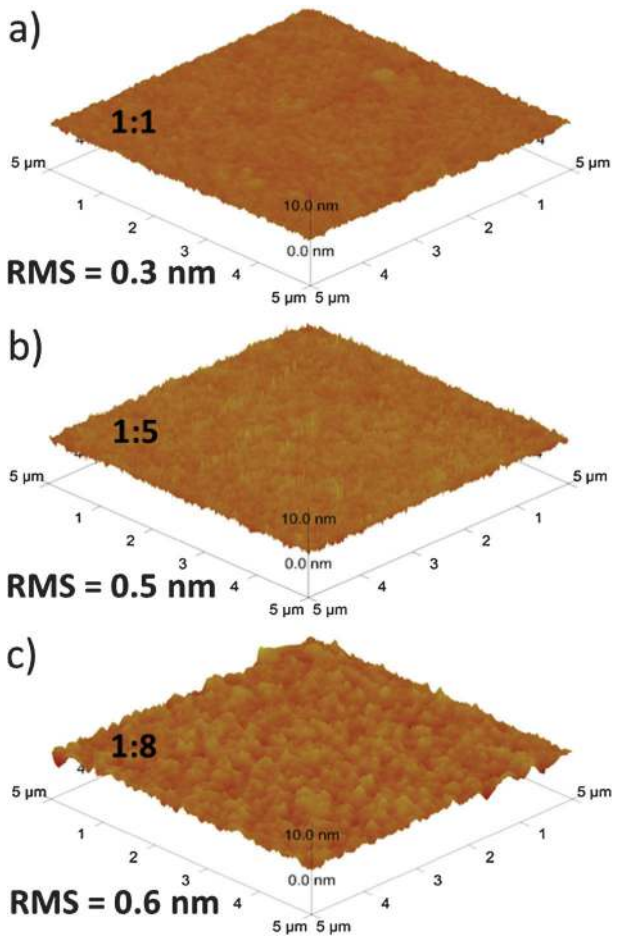

Fig. 5 AFM images (3-dimensional) of (a) 1 : 1 SQ : $PC_{70}BM$, (b) 1 : 5 SQ : $PC_{70}BM$, and (c) 1 : 8 SQ : $PC_{70}BM$ films spin-coated on MoO_3 coated ITO glass substrates.

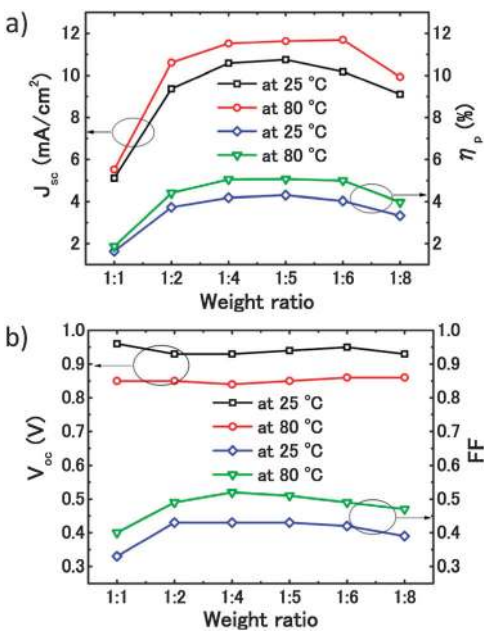

Fig. 6 Summary of key parameters of PV cells based on various SQ : $PC_{70}BM$ blending ratios at room temperature and 80 °C. (a) J_{sc} and η_p; (b) V_{oc} and FF.

For 1 : 5 ratio cells, J_{sc} increases from 10.8 mA cm^{-2} at room temperature to 11.6 mA cm^{-2} at 80 °C. Under illumination, the elevated temperature results in an increase in shunt resistance, and a decrease in serial resistance, as suggested in the *J–V* characteristics shown in Fig. S3a and S3b (ESI†). FF increases from 43% to 51%. Both the reduction of recombination loss and an increase in forward bias injection suggest an increase in carrier mobilities.[34] This is consistent with a uniform increase in EQE throughout the photoresponse range (see Fig. S3c, ESI†).

Table 2 PV performance for the SQ : $PC_{70}BM$ based solar cells at 80 °C

Weight ratio	J_{sc} (mA cm^{-2})	V_{oc} (V)	FF	η_p (%) (P_0 = 100 mW cm^{-2})
1 : 1	5.4 ± 0.1	0.84 ± 0.01	0.39 ± 0.01	1.7 ± 0.2
1 : 2	10.4 ± 0.2	0.84 ± 0.01	0.48 ± 0.01	4.1 ± 0.3
1 : 4	11.3 ± 0.2	0.83 ± 0.01	0.51 ± 0.01	4.7 ± 0.3
1 : 5	11.4 ± 0.2	0.84 ± 0.01	0.50 ± 0.01	4.8 ± 0.3
1 : 6	11.5 ± 0.2	0.85 ± 0.01	0.48 ± 0.01	4.7 ± 0.3
1 : 8	9.7 ± 0.2	0.85 ± 0.01	0.46 ± 0.01	4.7 ± 0.3
1 : 19	6.4 ± 0.2	0.86 ± 0.01	0.36 ± 0.01	2.0 ± 0.1
1 : 99	3.1 ± 0.1	0.89 ± 0.01	0.29 ± 0.01	0.8 ± 0.1

It was further confirmed *via* mobility characterization based on a space charge limited current model.[4]

3.5 Characterization of carrier mobility

For electron-only devices, a structure of ITO/Cs_2CO_3/SQ:$PC_{70}BM$/BCP/Al was used,[37] and 5 nm MoO_3 films were used as a buffer in hole-only devices.[24] Table 3 and Fig. S4 (ESI†) summarize mobility data at room temperature and 80 °C. SQ film from a solution process has a hole mobility of 3.54×10^{-5} cm^2 V^{-1} s^{-1}. Upon blending with $PC_{70}BM$, it drops further by one order of magnitude. At room temperature, the averaged values of electron and hole mobilities from multiple devices range about 10^{-4} and 10^{-5} cm^2 V^{-1} s^{-1}, respectively. At 80 °C, the hole mobilities increased by at least 2 times, while electron mobilities slightly increased. It agrees with the hopping model of charge transport in disordered materials, indicating that hole transport could be critical for charge extraction in SQ:$PC_{70}BM$ blend films. Even at 80 °C the optimal device shows FF ~50%, which is much below the state-of-the-art organic solar cells, suggesting huge room for improvement in PV performance from the SQ compound.[38,39]

3.6 Low donor concentration in bulk heterojunctions

As mentioned in Section 3.1, low donor ratio cells, *i.e.* 1 : 19 and 1 : 99, demonstrated an exceptionally large slope of V_{oc} *vs.* incident light intensity. In order to understand this phenomenon, $PC_{70}BM$-only cells were also fabricated. As shown in Table 1, the $PC_{70}BM$-only cell shows a high V_{oc} of 1.23 V (also Fig. S5, ESI†), which could be attributed to the difference in work function between an ITO/MoO_3 anode (−5.7 eV) and an Al cathode (−4.2 eV).[40] The contact between MoO_3 and $PC_{70}BM$ is responsible for the high V_{oc} as reported by Tang's group.[41] The cell shows an astonishing slope of $15kT/q$, which is dominated by the interface between MoO_3 and $PC_{70}BM$.[40] On the other hand, the photocurrent under 1 sun illumination is very low, suggesting that charge generation at interfaces and in the bulk film is very inefficient. In a cell with SQ : $PC_{70}BM$ (1 : 99), V_{oc} decreased from 1.23 to 1.01 V, whereas J_{sc} dramatically increased from 0.21 to 2.1 mA cm^{-2}, though absorption of SQ was negligible. Photoresponse of $PC_{70}BM$ from 350 nm to 600 nm kept increasing with increasing SQ loading (see Fig. S5c, ESI†), showing that donor molecules effectively improved free carrier generation in the $PC_{70}BM$ film through charge transfer. At the same time, V_{oc} drops down to ~0.95 V consistent with HOMO–LUMO offset between SQ and $PC_{70}BM$. The organic heterojunction starts to dominate the relationship between V_{oc} and incident light intensity.

3.7 Competitive OPV performance from as-synthesised SQ

As we pointed out in the synthesis part, purity of the as-synthesized SQ approaches 100% according to HPLC data. Regarding PV performance, the OPV cells based on sublimated and as-synthesized SQ delivered almost identical *J–V* characteristics and EQE spectra at both room temperature and 80 °C as shown in Fig. S6 (ESI†). Purification of the SQ compound *via* vacuum sublimation has no effects on both optical and electric properties of OPV cells. According to the mobility data (not shown), there are negligible differences in 1 : 5 ratio blend films based on SQ before and after sublimation. It demonstrates that the as-synthesized SQ compound can be directly used in solution processed OPV cells.

4. Conclusions

In summary, we have investigated characteristics of SQ based solution processed OPV cells, as well as related optoelectronic properties of materials and films. It was found that $\eta_p > 4.0\%$ can be obtained. Interestingly the OPV cells show higher η_p at an elevated operation temperature of 80 °C, which is ascribed to enhanced carrier mobilities. As-synthesized SQ shows competitive η_p, indicating that SQ and its analogs are easy-to-purify compounds, and thus promising materials for future applications in OPVs.

Acknowledgements

This project is sponsored by the Japan Science and Technology Agency (JST) *via* the Japan Regional Innovation Strategy Program by the Excellence (J-RISE), and Adaptable and Seamless Technology transfer Program (A-STEP, No. AS232Z00929D). The authors would like to thank Prof. K. Nakayama, Dr D. Yokoyama for technical support and scientific discussion, and Dr J. Y. Hu, Dr C. Cai, Dr T. Motoyama, Mr Y. Maruya, Mr Y. Kawata and Ms H. Nakanishi, Mr Y. Ueno for technical assistance. ZH thanks W. Tress for scientific discussion.

Table 3 Carrier mobility data derived from a space charge limited current model

Weight ratio	SQ	1 : 1	1 : 2	1 : 4	1 : 5	1 : 6	1 : 8	$PC_{70}BM$
μ_h (25 °C) (cm^2 V^{-1} s^{-1})	3.54×10^{-5}	2.36×10^{-5}	1.53×10^{-5}	1.39×10^{-5}	2.07×10^{-5}	1.37×10^{-5}	6.55×10^{-6}	—
μ_h (80 °C) (cm^2 V^{-1} s^{-1})	5.59×10^{-5}	3.27×10^{-5}	2.42×10^{-5}	3.21×10^{-5}	2.93×10^{-5}	2.86×10^{-5}	1.76×10^{-5}	—
μ_e (25 °C) (cm^2 V^{-1} s^{-1})	—	2.99×10^{-5}	7.15×10^{-4}	4.38×10^{-4}	3.66×10^{-4}	7.35×10^{-4}	7.10×10^{-4}	8.54×10^{-4}
μ_e (80 °C) (cm^2 V^{-1} s^{-1})	—	9.95×10^{-5}	9.75×10^{-4}	5.68×10^{-4}	4.25×10^{-4}	9.57×10^{-4}	9.46×10^{-4}	1.65×10^{-3}

Notes and references

1 B. Azzopardi, C. J. M. Emmott, A. Urbina, F. C. Krebs, J. Mutale and J. Nelson, *Energy Environ. Sci.*, 2011, **4**, 3741.
2 C. W. Tang, *Appl. Phys. Lett.*, 1986, **48**, 183.
3 G. Yu, J. Gao, J. C. Hummelen, F. Wudl and A. J. Heeger, *Science*, 1995, **270**, 1789.
4 P. W. M. Blom, V. D. Mihailetchi, L. J. A. Koster and D. E. Markov, *Adv. Mater.*, 2007, **19**, 1551.
5 X. D. Dang, A. B. Tamayo, J. Seo, C. V. Hoven, B. Walker and T. Q. Nguyen, *Adv. Funct. Mater.*, 2010, **20**, 3314.
6 E. Ronchi, R. Ruffo, S. Rizzato, A. Albinati, L. Beverina and G. A. Pagani, *Org. Lett.*, 2011, **13**, 3166.
7 F. Würthner, T. E. Kaiser and C. R. Saha-Möller, *Angew. Chem., Int. Ed.*, 2011, **50**, 3376.
8 G. D. Wei, S. Y. Wang, K. Renshaw, M. E. Thompson and S. R. Forrest, *ACS Nano*, 2010, **4**, 1927.
9 (*a*) S. Y. Wang, E. I. Mayo, M. D. Perez, L. Griffe, G. D. Wei, P. I. Djurovich, S. R. Forrest and M. E. Thompson, *Appl. Phys. Lett.*, 2009, **94**, 233304; (*b*) G. Chen, D. Yokoyama, H. Sasabe, Z. R. Hong, Y. Yang and J. Kido, *Appl. Phys. Lett.*, 2012, **101**, 083904.
10 G. D. Wei, S. Y. Wang, K. Sun, M. E. Thompson and S. R. Forrest, *Adv. Energy Mater.*, 2011, **1**, 184.
11 G. Chen, H. Sasabe, Z. Q. Wang, X. F. Wang, Z. R. Hong, Y. Yang and J. Kido, *Adv. Mater.*, 2012, **24**, 2768.
12 U. Mayerhöffer, K. Deing, K. Gruss, H. Braunschweig, K. Meerholz and F. Würthner, *Angew. Chem., Int. Ed.*, 2009, **48**, 8776.
13 K. C. Deing, U. lrich Mayerhöffer, F. Würthner and Klaus Meerholz, *Phys. Chem. Chem. Phys.*, 2012, **14**, 8328.
14 L. Beverina, R. Ruffo, M. M. Salamone, E. Ronchi, M. Binda, D. Natali and M. Sampietro, *J. Mater. Chem.*, 2012, **22**, 6704.
15 S. R. Forrest, *Chem. Rev.*, 1997, **97**, 1793.
16 H. Y. Chen, J. H. Hou, S. Q. Zhang, Y. Y. Liang, G. W. Yang, Y. Yang, L. P. Yu, Y. Wu and G. Li, *Nat. Photonics*, 2009, **3**, 649.
17 Y. J. He and Y. F. Li, *Phys. Chem. Chem. Phys.*, 2011, **13**, 1970.
18 A. Ojala, H. Bürckstümmer, M. Stolte, R. Sens, H. Reichelt, P. Erk, J. Hwang, D. Hertel, K. Meerholz and F. Würthner, *Adv. Mater.*, 2011, **23**, 5398.
19 Y. S. Liu, X. J. Wan, F. Wang, J. Y. Zhou, G. K. Long, J. G. Tian, J. B. You, Y. Yang and Y. S. Chen, *Adv. Energy Mater.*, 2011, **1**, 771.
20 J. Gilot, M. M. Wienk and R. A. J. Janssen, *Adv. Mater.*, 2010, **22**, E67.
21 S. Sista, Z. R. Hong, M. H. Park, Z. Xu and Y. Yang, *Adv. Mater.*, 2010, **22**, E77.
22 M. Q. Tian, M. Furuki, I. Iwasa, Y. Sato, L. S. Pu and S. Tatsuura, *J. Phys. Chem. B*, 2002, **106**, 4370.
23 C. W. Dirk, W. C. Herndon, F. Cervantes-Lee, H. Selnau, S. Martinez, P. Kalamegham, A. Tan, G. Campos, M. Velez, J. Zyss, I. Ledoux and L. T. Cheng, *J. Am. Chem. Soc.*, 1995, **117**, 2214.
24 V. Shrotriya, G. Li, Y. Yao, C. W. Chu and Y. Yang, *Appl. Phys. Lett.*, 2006, **88**, 073508.
25 P. Peumans, A. Yakimov and S. R. Forrest, *J. Appl. Phys.*, 2003, **93**, 3693.
26 I. Hancox, K. V. Chauhan, P. Sullivan, R. A. Hatton, A. Moshar, C. P. A. Mulcahy and T. S. Jones, *Energy Environ. Sci.*, 2010, **3**, 107.
27 Y. Sun, C. J. Takacs, S. R. Cowan, J. H. Seo, X. Gong, A. Roy and A. J. Heeger, *Adv. Mater.*, 2011, **23**, 2226.
28 M. H. Chen, J. H. Hou, Z. R. Hong, G. W. Yang, S. Sista, L. M. Chen and Y. Yang, *Adv. Mater.*, 2009, **21**, 4238.
29 L. J. A. Koster, V. D. Mihailetchi, R. Ramaker and P. W. M. Blom, *Appl. Phys. Lett.*, 2011, **86**, 123509.
30 G. A. H. Wetzelaer, L. J. A. Koster and P. W. M. Blom, *Phys. Rev. Lett.*, 2011, **107**, 066605.
31 G. Li, V. Shrotriya, J. Huang, Y. Yao, T. Moriarty, K. Emery and Y. Yang, *Nat. Mater.*, 2005, **4**, 864.
32 B. Yang, J. Cox, Y. Yuan, F. Guo and J. Huang, *Appl. Phys. Lett.*, 2011, **99**, 133302.
33 http://www.pveducation.org/pvcdrom/solar-cell-operation/effect-of-temperature.
34 C. Deibel and V. Dyakonov, *Rep. Prog. Phys.*, 2010, **73**, 096401.
35 G. Garcia-Belmonte, *Sol. Energy Mater. Sol. Cells*, 2010, **94**, 2166.
36 J. Nelson, *the Physics of Solar cells, ISBN 1-86094-340-3*, Imperial College Press: London, U.K., 2003.
37 G. Li, C. W. Chu, V. Shrotriya, J. Huang and Y. Yang, *Appl. Phys. Lett.*, 2006, **88**, 253503.
38 L. J. Huo, J. H. Hou, S. Q. Zhang, H. Y. Chen and Y. Yang, *Angew. Chem., Int. Ed.*, 2010, **49**, 1500.
39 Y. Sun, G. C. Welch, W. L. Leong, C. J. Takacs, G. C. Bazan and A. J. Heeger, *Nat. Mater.*, 2012, **11**, 44.
40 M. L. Zhang, Irfan, H. J. Ding, Y. L. Gao and C. W. Tang, *Appl. Phys. Lett.*, 2010, **96**, 183301.
41 M. L. Zhang, H. Wang, H. K. Tian, Y. H. Geng and C. W. Tang, *Adv. Mater.*, 2011, **23**, 4960.

